

# Benchmark Elasticity Solution for Locally Loaded Laminated Orthotropic Cylindrical Shells

K. Bhaskar\* and T. K. Varadan†

*Indian Institute of Technology, Madras 600 036, India*

Three-dimensional elasticity solutions for plate/shell structures serve as a standard benchmark for the assessment of various two-dimensional theories. Such a solution, for assessment of laminated shell theories, is presented here. The problem is that of a simply supported cross-ply cylindrical shell pinched by two diametrically opposite local patch loads. The solution is developed by using Taylor series, and results are tabulated for a three-layer shell with various radius-to-thickness ratios. Finally, these results are used to throw light on the accuracy of the classical Love-Kirchhoff hypothesis and a recently proposed higher order shear deformation theory.

## Introduction

**P**LATES and shells, which are essentially three-dimensional structures, are usually analyzed by two-dimensional theories wherein the variation of the displacements (and stresses) through the thickness of the plate/shell is assumed a priori. Based on the type of variation assumed, one has a variety of plate/shell theories. However, all of these theories are but approximations to the three-dimensional reality and, as such, have to be justified with regard to their accuracy. An assessment of the accuracy of two-dimensional theories is possible only by comparison with rigorous three-dimensional analysis for at least some simple test cases. Such a test case, for assessment of laminated composite shell theories, is the topic of the present work.

The inadequacy of the classical Love-Kirchhoff hypothesis of nondeformable normals for structures laminated of fiber-reinforced layers has been well recognized.<sup>1</sup> Because of the low ratio of the transverse shear modulus to the in-plane Young's moduli that is typical of a composite lamina, transverse shear deformation effects have to be accounted for, and hence a variety of laminate theories, ranging from the simple Mindlin-type first-order approach to complex multivariable individual layer approaches, have appeared in the literature.

Coupled with this, there has been a growing interest in three-dimensional solutions for laminates, and a number of simple test cases have been analyzed using the rigorous elasticity approach. Although such benchmark results for laminated composite plates have been available for about two decades now,<sup>2-6</sup> three-dimensional solutions of laminated fiber-reinforced shells are of more recent origin. Ren<sup>7</sup> considered the plane strain deformation of transversely loaded simply supported cross-ply cylindrical shell strips using a stress-function approach and provided results in the form of maximum displacements and stresses for various stacking sequences. The more general case of finite length cross-ply cylindrical shells subjected to transverse loading varying sinusoidally in both the axial and circumferential directions was analyzed later by employing the Frobenius power series method.<sup>8,9</sup> Elasticity solutions have also been obtained recently for simply supported angle-ply cylindrical shells undergoing 1) bending in the circumferential direction alone, i.e., the generalized plane strain problem,<sup>10</sup> and 2) axisymmetric deformation.<sup>11</sup> An exact closed-form solution has been obtained in the first case, whereas the second case has been analyzed by using Taylor

series. All of the references discussed earlier present results for (smoothly varying) sinusoidally distributed transverse loads (in addition, a central band load was also considered for the axisymmetrically loaded angle-ply shell in Ref. 11).

The presence of discontinuous or locally applied loads leads to steeper stress gradients and presents a more critical test case for the assessment of shell theories. Further, since failure often initiates at such high stress locations, it is essential that a shell theory gives accurate stress estimates at these critical zones for it to be considered useful. Thus there is a need to assess the accuracy of shell theories for problems involving local loads, and hence standard benchmark solutions for some such problems are required.

It is in this context that the present work addresses the well-known problem of a circular cylindrical shell pinched by diametrically opposite loads. Each load acts on a small rectangular patch, and the shell is assumed to be made of specially orthotropic layers and with the ends supported by shear diaphragms. The problem is analyzed by expanding the load in a double Fourier series in the two surface coordinates of the shell and by summing the results for each Fourier harmonic. At this stage it is shown that the methodology based on Frobenius power series presented earlier for sinusoidal transverse loading<sup>9</sup> leads to numerical difficulties when the wave numbers are high, and hence it cannot be used for consideration of local loads. Hence an alternative solution, based on simple Taylor series, is first presented for sinusoidal loading and then used with Fourier summation to yield results for the present problem. Numerical results are tabulated for a three-layer shell for a set of radius-to-thickness ratios. Finally, in the light of these results, the accuracy of two shell theories—one based on the classical Love-Kirchhoff hypothesis and the other on a higher order displacement field—is examined.

## Formulation

A laminated cylindrical shell as shown in Fig. 1 is considered. The variables  $R_{\max}$ ,  $R_0$ ,  $h$ , and  $L$  denote the maximum radius, mean radius, thickness, and length of the shell, respectively. The  $N$  layers of the shell are oriented such that the material axes of any layer are aligned with the  $\theta$ - $z$  directions, i.e., the shell is "laminated orthotropic." The shell is subjected to pinching loads,  $P$  each, acting on two diametrically opposite rectangular patches on the outer surface as shown. The two circular ends are assumed to be supported by shear diaphragms, i.e., at  $z = 0, L$ ,

$$\sigma_z = u_r = u_\theta = 0 \quad (1)$$

where  $u$  denotes the displacement along a coordinate direction.

The governing equations of the three-dimensional boundary-value problem are the following:

Received March 24, 1993; revision received Aug. 23, 1993; accepted for publication Aug. 23, 1993. Copyright © 1993 by the American Institute of Aeronautics and Astronautics, Inc. All rights reserved.

\*Assistant Professor, Department of Aerospace Engineering.

†Professor, Department of Aerospace Engineering.

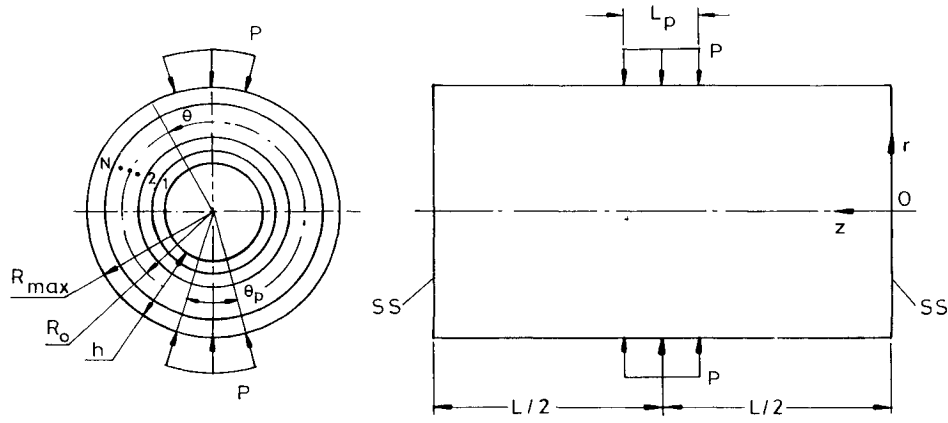


Fig. 1 Pinched cylindrical shell.

1) Equilibrium equations:

$$\begin{aligned}\sigma_{r,r} + \tau_{r\theta,\theta}/r + \tau_{rz,z} + (\sigma_r - \sigma_\theta)/r &= 0 \\ \tau_{r\theta,r} + \sigma_{\theta,\theta}/r + \tau_{\theta z,z} + 2\tau_{r\theta}/r &= 0 \\ \tau_{rz,r} + \tau_{\theta z,\theta}/r + \sigma_{z,z} + \tau_{rz}/r &= 0\end{aligned}\quad (2)$$

2) Stress-strain law:

$$\begin{Bmatrix} \sigma_r \\ \sigma_\theta \\ \sigma_z \end{Bmatrix} = \begin{bmatrix} C_{11} & C_{12} & C_{13} \\ & C_{22} & C_{23} \\ \text{sym} & & C_{33} \end{bmatrix} \begin{Bmatrix} \epsilon_r \\ \epsilon_\theta \\ \epsilon_z \end{Bmatrix}; \quad \begin{aligned} \tau_{rz} &= C_{44}\gamma_{rz} \\ \tau_{r\theta} &= C_{55}\gamma_{r\theta} \\ \tau_{\theta z} &= C_{66}\gamma_{\theta z} \end{aligned}\quad (3)$$

where  $C_{ij}$  are the stiffness coefficients of the layer under consideration.

3) Strain-displacement relations:

$$\begin{aligned}\epsilon_r &= u_{r,r}, & \epsilon_\theta &= (u_{\theta,\theta} + u_r)/r, & \epsilon_z &= u_{z,z} \\ \gamma_{rz} &= u_{z,r} + u_{r,z}, & \gamma_{\theta z} &= u_{\theta,z} + u_{z,\theta}/r \\ \gamma_{r\theta} &= (u_{r,\theta} - u_{\theta,r})/r + u_{\theta,r}\end{aligned}\quad (4)$$

The boundary conditions to be satisfied, besides those of Eq. (1), are those at the lateral surfaces and interfaces between the layers of the shell. These are given as follows:

At the inner surface:

$$\sigma_r = \tau_{r\theta} = \tau_{rz} = 0 \quad (5a)$$

At the outer surface:

$$\sigma_r = -q_0, \quad \tau_{r\theta} = \tau_{rz} = 0 \quad (5b)$$

At the interface between  $i$ th and  $(i+1)$ th layers:

$$\begin{aligned}(\sigma_r, \tau_{r\theta}, \tau_{rz}, u_r, u_\theta, u_z) & \quad \text{for } i\text{th layer} \\ &= (\sigma_r, \tau_{r\theta}, \tau_{rz}, u_r, u_\theta, u_z) \quad \text{for } (i+1)\text{th layer}\end{aligned}\quad (5c)$$

In Eqs. (5),  $q_0$  stands for the load per unit area corresponding to the pinching patch loads;  $q_0$  is obtained by using a double Fourier summation along  $\theta, z$  directions as

$$q_0(\theta, z) = \sum_m \sum_n [Q_{mn} \sin m\pi z/L \cos n\theta] \quad (6)$$

where  $m = 1, 3, 5, \dots, n = 0, 2, 4, \dots$ ,

$$Q_{m0} = (4P/\pi^2 m L_p R_{\max}) \sin(m\pi L_p/2L) \sin(m\pi/2)$$

and for  $n \geq 2$ ,

$$Q_{mn} = (16P/\pi^2 m n L_p R_{\max} \theta_p) \sin(m\pi L_p/2L) \sin(m\pi/2) \sin(n\theta_p/2)$$

where  $R_{\max}\theta_p$  and  $L_p$  denote the dimensions of the load patch as shown in Fig. 1.

### Solution

The first step is to reduce the boundary-value problem to a set of ordinary differential equations in terms of the radial coordinate. Considering only one harmonic (or  $m, n$  combination) of the applied load at a time, one can assume that the displacements vary harmonically in  $\theta$  and  $z$  directions as

$$\begin{aligned}u_r &= h \phi_r \sin m\pi z/L \cos n\theta \\ u_\theta &= h \phi_\theta \sin m\pi z/L \sin n\theta \\ u_z &= h \phi_z \cos m\pi z/L \cos n\theta\end{aligned}\quad (7)$$

where  $\phi_r, \phi_\theta$ , and  $\phi_z$  are functions of  $r$  alone. These expressions satisfy Eq. (1) and can be used along with Eqs. (3) and (4) to reduce Eq. (2) to the following coupled homogeneous ordinary differential equations in  $r$ :

$$\begin{aligned}[C_{11}D_2 + C_{11}D_1/r - (C_{55}n^2 + C_{22})/r^2 - C_{44}(m\pi/L)^2]\phi_r \\ + [(C_{55} + C_{12})nD_1/r - (C_{55} + C_{22})n/r^2]\phi_\theta \\ + [-(C_{13} + C_{44})(m\pi/L)D_1 \\ - (C_{13} + C_{23})(m\pi/L)/r]\phi_z = 0\end{aligned}\quad (8a)$$

$$\begin{aligned}[-(C_{55} + C_{12})nD_1/r - (C_{55} + C_{22})n/r^2]\phi_r \\ + [C_{55}(D_2 + D_1/r) - (C_{22}n^2 + C_{55})/r^2 - C_{66}(m\pi/L)^2]\phi_\theta \\ + [(C_{23} + C_{66})n(m\pi/L)/r]\phi_z = 0\end{aligned}\quad (8b)$$

$$\begin{aligned}[(C_{44} + C_{13})(m\pi/L)D_1 + (C_{44} + C_{23})(m\pi/L)/r]\phi_r \\ + [(C_{66} + C_{23})n(m\pi/L)/r]\phi_\theta \\ + [C_{44}(D_2 + D_1/r) - C_{66}n^2/r^2 - C_{33}(m\pi/L)^2]\phi_z = 0\end{aligned}\quad (8c)$$

where  $D_2 = d^2/dr^2$ , and  $D_1 = d/dr$ .

This system of differential equations has a regular singular point at  $r = 0$  and permits a solution in terms of a Frobenius power series<sup>12</sup> for  $\phi_r, \phi_\theta$ , and  $\phi_z$ , i.e.,

$$(\phi_r, \phi_\theta, \phi_z) = \sum_{j=0}^{\infty} r^{\alpha+j} [\bar{\phi}_r(j), \bar{\phi}_\theta(j), \bar{\phi}_z(j)] \quad (9)$$

where  $\alpha$  is an unknown nonintegral exponent, and  $\bar{\phi}_r$ , etc., are unknown coefficients. Substituting Eq. (9) into Eq. (8) and equating the coefficient of each power of  $r$  to zero yield six values of  $\alpha$ . Corresponding to each value of  $\alpha$ ,  $\bar{\phi}_r(j)$ ,  $\bar{\phi}_\theta(j)$ , and  $\bar{\phi}_z(j)$  ( $j = 0$  to  $\infty$ ) can be obtained in terms of one

undetermined constant. Thus there are six undetermined constants per layer or  $6N$  for the shell that can be obtained by utilizing the lateral surface and interface conditions [Eqs. (5)]. This type of solution has been presented earlier<sup>8,9</sup> for bending of laminated orthotropic cylindrical shells due to sinusoidally distributed transverse loading. This type of approach, based on the Frobenius series, was also used much earlier for free vibration analysis of single-layer<sup>13,14</sup> and multilayered orthotropic shells.<sup>15</sup>

Though the Frobenius method leads to a convergent series solution and can be used to obtain results of any desired accuracy, one encounters numerical difficulties in practice when higher harmonics (or  $m, n$  values) are considered. The system of algebraic equations (arising from the lateral and interface boundary conditions) to determine the  $6N$  unknown arbitrary constants becomes highly ill-conditioned so that small changes in the values of the coefficients lead to large changes in the solution. Hence the power series has to be summed to a great degree of accuracy, which is limited by the numerical precision of the computer used. For example, double precision arithmetic (with 18 mantissa digits on a Siemens 7580-E computer) has been found to yield nonconvergent (and physically absurd) results even for low values of  $m, n$ , viz., 1 and 4, respectively,<sup>9</sup> and correct, converged results are possible only with quadruple precision arithmetic (with 34 mantissa digits). For  $m$  or  $n > 8$ , even quadruple precision has been found to be inadequate.

These numerical difficulties are not entirely unforeseen. In fact, they have been reported earlier in connection with the analysis of homogeneous orthotropic cylindrical shells.<sup>14,16</sup> As an alternative approach, a perturbation solution was developed in Ref. 16.

In the present work, a Taylor series solution is developed as a way out of the numerical difficulties encountered in the Frobenius approach. This is achieved by developing a power series solution not around the singular point at  $r = 0$  but around the ordinary (nonsingular) point at  $r = R_0$ . For the sake of convenience, a new radial coordinate is defined as

$$\xi = 2(r - R_0)/h \quad (10)$$

In terms of  $\xi$ , Eqs. (8a-8c) get transformed as

$$\begin{aligned} & [C_{11}(\xi + t)^2 \bar{D}_2 + C_{11}(\xi + t) \bar{D}_1 - C_{55}n^2 - C_{22} \\ & - C_{44}s^2(\xi + t)^2] \phi_r + [(C_{55} + C_{12})n(\xi + t) \bar{D}_1 \\ & - (C_{55} + C_{22})n] \phi_\theta - [(C_{13} + C_{44})s(\xi + t)^2 \bar{D}_1 \\ & + (C_{13} - C_{23})(\xi + t)s] \phi_z = 0 \end{aligned} \quad (11a)$$

$$\begin{aligned} & - [(C_{55} + C_{12})n(\xi + t) \bar{D}_1 + (C_{55} + C_{22})n] \phi_r \\ & + [C_{55}(\xi + t)^2 \bar{D}_2 + C_{55}(\xi + t) \bar{D}_1 - (C_{22}n^2 + C_{55}) \\ & - C_{66}s^2(\xi + t)^2] \phi_\theta + (C_{23} + C_{66})ns(\xi + t) \phi_z = 0 \end{aligned} \quad (11b)$$

$$\begin{aligned} & [(C_{44} + C_{13})s(\xi + t)^2 \bar{D}_1 + (C_{44} + C_{23})s(\xi + t)] \phi_r \\ & + [(C_{66} + C_{23})ns(\xi + t)] \phi_\theta + [C_{44}(\xi + t)^2 \bar{D}_2 \\ & + C_{44}(\xi + t) \bar{D}_1 - C_{66}n^2 - C_{33}s^2(\xi + t)^2] \phi_z = 0 \end{aligned} \quad (11c)$$

where  $\bar{D}_2 = d^2/d\xi^2$ ,  $\bar{D}_1 = d/d\xi$ ,  $s = m\pi h/2L$ , and  $t = 2R_0/h$ .

Equations (11a-11c) have a power series solution about the ordinary point  $\xi = 0$  given by<sup>12</sup>

$$(\phi_r, \phi_\theta, \phi_z) = \sum_{j=0,1,2,\dots}^{\infty} \xi^j [H_r(j), H_\theta(j), H_z(j)] \quad (12)$$

where  $H_r$  to  $H_z$  are unknown coefficients. Substituting Eqs. (12) into Eq. (11) and equating the coefficient of each power

of  $\xi$  yield the values of  $H_r$ ,  $H_\theta$ , and  $H_z$  in terms of six undetermined constants  $G(k)$ ,  $k = 1-6$ , i.e., for  $j = 0$  to  $\infty$ ,

$$[H_r(j), H_\theta(j), H_z(j)] = \sum_{k=1}^6 G(k) [d_r(j, k), d_\theta(j, k), d_z(j, k)] \quad (13)$$

where  $d_r$ ,  $d_\theta$ , and  $d_z$  are defined in the Appendix.

Equations (12) and (13) give the values of  $\phi_r$ ,  $\phi_\theta$ , and  $\phi_z$  at any point of the layer under consideration in terms of  $G(k)$ ,  $k = 1-6$ . Thus, for the  $N$ -layered shell, there would be  $6N$  undetermined constants, say  $G(i, k)$ ,  $i = 1-N$ ,  $k = 1-6$ . The displacements, strains, and stresses are then obtained in terms of  $G(i, k)$  from Eqs. (7), (4), and (3), respectively. Finally, the  $6N$  conditions of Eqs. (5) yield a system of  $6N$  algebraic equations to determine the constants  $G(i, k)$ .

## Results and Discussion

To start with, the utility of the present solution for high values of  $m$  and  $n$  has to be established. With this in view, (90/0)- and (90/0/90)-deg shells (with equal thickness layers, the fiber orientation of the outer layer being specified first and orientation being measured in degrees with respect to the  $z$  axis) subjected to transverse harmonic loading are studied first. The  $L/R_0$  is taken as 4 and the material properties of the layers are taken to be  $E_L/E_T = 25$ ,  $G_{LT}/E_T = 0.5$ ,  $G_{TT}/E_T = 0.2$ , and  $\nu_{LT} = \nu_{TT} = 0.25$ .

Values of  $R_0/h$  ranging from 10 to 100 are considered. Starting from small values,  $m$  and  $n$  are both increased gradually. For all of these cases, the power series is summed until results converge to the fifth significant digit. All calculations are performed in quadruple precision on a Siemens 7580-E computer. It is found from this study that the present method remains free of ill-conditioning or other numerical difficulties even for values of  $m$  and  $n$  as high as 140 (whereas the Frobenius method fails for  $m$  or  $n$  as low as 9). Though numerical difficulties due to ill-conditioning are inherent to any power series solution and will arise in the present approach also if very high values of  $m$  and  $n$  are considered, the fact that Fourier summation up to  $m = n = 140$  is possible with the present method makes it useful for consideration of localized patch loads.

Having established the utility of the Taylor series solution for high harmonics, we now apply it to the problem of the pinched cylinder. A (90/0/90)-deg shell with  $L/R_0 = 4$  and material properties as given earlier is considered. The patch size is taken to be  $L_p/L = \theta_p/\pi = 1/25$ . For this size it is found that results converge well with  $m = 1, 3, \dots, 49$  and  $n = 0, 2, \dots, 48$ . Increasing  $m_{\max}$  and  $n_{\max}$  to 59 and 58, respectively, changes the results very marginally (deflections by less than 0.1% and all stresses except  $\sigma_r$  by less than 2%). Hence  $(m_{\max}, n_{\max}) = (49, 48)$  is considered adequate for the present problem.

The results for  $R_0/h = 10, 20, 50$ , and 100 are presented in Table I in terms of the following nondimensional parameters:

$$\bar{U}_r = E_L h u_r / P$$

$$(\bar{\sigma}_\alpha \text{ or } \bar{\tau}_{\alpha\beta}) = h^2 (\sigma_\alpha \text{ or } \tau_{\alpha\beta}) / P \text{ for } \alpha, \beta = r, \theta, z$$

All of the stresses reach their maximum values directly under the load patch but at different points within the patch area. The exact locations are also mentioned in Table I. Further, to give an idea as to how the deflection varies as one moves away from the load patch, values of  $\bar{U}_r$  on the middle surface of the shell at different  $\theta, z$  locations are presented in Table 2. These results, along with the exact solutions presented earlier,<sup>7-11</sup> form a useful set of benchmark cases for assessing the validity of various thicknesswise approximations employed in two-dimensional shell theories.

As an illustration, the accuracy of the Love-Kirchhoff hypothesis is assessed by comparison with the elasticity solution. The classical shell theory based on the Love-Kirchhoff hypothesis but not involving any further assumptions or simplifi-

Table 1 Deflections and stresses in a pinched (90/0/90)-deg shell

$R_0/h$	$\xi^a$	$\bar{U}_r$	$10\bar{\sigma}_r$	$\bar{\sigma}_\theta$	$\bar{\sigma}_z$	$10\bar{\tau}_{rz}$	$10\bar{\tau}_{\theta z}$	$10\bar{\tau}_{r\theta}$
10	-1	-93.43	0	3.485	0.358	0	0.7721	0
	-3/4	-93.79	-0.341	0.621	0.172	-0.594	0.4265	2.056
	-1/2	-94.24	-1.363	-1.178	0.040	-0.860	0.2552	1.661
				-0.059	2.100			
	0	-95.01	-2.555	-0.057	-0.260	-2.422	0.2486	1.595
	1/4	-96.22	-3.787	-0.087	-2.714	-1.169	0.1985	1.584
				0.734	-0.191			
	3/4	-97.77	-5.156	-1.541	-0.332	-0.810	0.0152	2.838
	1	-99.64	-6.583	-5.488	-0.622	0	-0.5658	0
20	-1	-169.1	0	2.447	0.228	0	0.5869	0
	-3/4	-169.3	-0.031	0.779	0.128	-0.248	0.3758	1.085
	-1/2	-169.5	-0.295	-0.435	0.042	-0.379	0.2244	1.077
				-0.011	1.343			
	0	-169.7	-0.642	-0.031	-0.307	-1.088	0.1602	1.066
	1/4	-169.9	-0.986	-0.054	-1.977	-0.377	0.0930	1.056
				-0.292	-0.105			
	3/4	-170.2	-1.340	-1.546	-0.196	-0.249	-0.0630	1.123
	1	-170.5	-1.686	-3.265	-0.310	0	-0.2905	0
50	-1	-351.3	0	1.543	0.113	0	0.4044	0
	-3/4	-351.4	0.0183	0.757	0.068	-0.0631	0.3045	0.3805
	-1/2	-351.5	-0.0108	0.072	0.025	-0.1014	0.2151	0.5186
				0.009	0.618			
	0	-351.5	-0.0682	-0.016	-0.268	-0.2839	0.1490	0.5258
	1/4	-351.5	-0.1255	-0.040	-1.157	-0.0785	0.0835	0.5254
				-0.655	-0.055			
	3/4	-351.4	-0.1993	-1.328	-0.100	-0.0516	-0.0056	0.3788
	1	-351.3	-0.2738	-2.093	-0.147	0	-0.1044	0
100	-1	-664.5	0	1.171	0.0633	0	0.3375	0
	-3/4	-664.6	0.0111	0.660	0.0379	-0.0218	0.2736	0.1718
	-1/2	-664.6	0.0081	0.177	0.0127	-0.0360	0.2123	0.2605
				0.010	0.2719			
	0	-664.6	-0.0053	-0.011	-0.2388	-0.0896	0.1573	0.2661
	1/4	-664.6	-0.0188	-0.032	-0.7504	-0.0218	0.1026	0.2672
				-0.614	-0.0363			
	3/4	-664.5	-0.0426	-1.092	-0.0620	-0.0147	-0.0415	0.1737
	1	-664.4	-0.0688	-1.593	-0.0883	0	-0.0219	0

<sup>a</sup>( $\theta, z$ ) values for the points at which the parameters are calculated are (0,  $L/2$ ) for  $\bar{U}_r, \bar{\sigma}_r, \bar{\sigma}_\theta, \bar{\sigma}_z$ ;  $[0, (L - L_p)/2]$  for  $\bar{\tau}_{rz}$ ;  $[\theta_p/2, (L - L_p)/2]$  for  $\bar{\tau}_{\theta z}$ ; and  $[\theta_p/2, L/2]$  for  $\bar{\tau}_{r\theta}$ .

Table 2 Deflections of the mean surface of a pinched (90/0/90)-deg shell

Location ( $\theta, z$ )	$\bar{U}_r$ at $\xi = 0$ for			
	$R_0/h = 10$	$R_0/h = 20$	$R_0/h = 50$	$R_0/h = 100$
(0, 0.3L)	-27.39	-58.79	-110.97	-201.62
(0, 0.4L)	-45.80	-87.79	-170.99	-316.59
(0, 0.5L)	-95.01	-169.66	-351.48	-664.63
( $\pi/4$ , 0.5L)	10.62	25.00	80.80	180.45
( $\pi/2$ , 0.5L)	46.05	76.95	77.55	3.34

Table 3 Results based on classical Love-Kirchhoff hypothesis

Item	Pinching patch loads		Internal sinusoidal pressure ( $m = 1, n = 4$ )	
	$R_0/h = 100$	$R_0/h = 50$	$R_0/h = 100$	$R_0/h = 50$
$u_r$	0.97 <sup>a,b</sup>	0.93	0.99 <sup>c</sup>	0.95
$\sigma_\theta$	0.98	0.94	1.00	0.99
$\sigma_z$	0.96	0.91	0.99	0.95
$\tau_{\theta z}$	0.93	0.82	0.99	0.96

<sup>a</sup>All values are normalized with respect to the corresponding elasticity results.  
<sup>b</sup>For the pinched cylinder, ( $\theta, z$ ) locations are as given in Table 1;  $\xi$  locations are 0 for  $u_r$ , 1 for  $\sigma_\theta$ ,  $1/2$  for  $\sigma_z$ , and  $-1$  for  $\tau_{\theta z}$ .  
<sup>c</sup>For the cylinder subjected to sinusoidal pressure, ( $\theta, z$ ) locations are such that the sine or cosine functions [see Eq. (7)] take maximum values;  $\xi$  locations are 0 for  $u_r$ ,  $1/2$  for  $\sigma_z$ , and  $-1$  for  $\sigma_\theta$  and  $\tau_{\theta z}$ .

Table 4 Results based on higher order shell theory

Item	$R_0/h = 100$	$R_0/h = 50$	$R_0/h = 20$	$R_0/h = 10$
$u_r$	1.00 <sup>a,b</sup>	1.00	1.00	1.00
$\sigma_\theta$	1.00	1.00	0.96	0.79
$\sigma_z$	1.00	1.00	1.01	1.03
$\tau_{\theta z}$	1.00	1.00	1.03	1.17

<sup>a,b</sup>As in Table 3.

cations has been presented by Bert.<sup>17</sup> This theory is used for the present problem with the Fourier expansion truncated again at  $m, n = 49$  and  $48$ , respectively. The maximum deflection and stresses predicted by the classical theory are normalized with respect to the elasticity solution and presented in Table 3, which also includes this sort of comparison for the case of a sinusoidally distributed transverse load with  $m = 1$  and  $n = 4$ , for which the elasticity results have been provided earlier.<sup>9</sup> Values of  $R_0/h$  below 50 are not considered because the classical theory has been proved to be highly inaccurate for such shells even when the load is sinusoidally distributed.<sup>8</sup> It can be seen from Table 3 that the accuracy of the Love-Kirchhoff hypothesis drops as the load is varied from a smoothly distributed one to a localized one. Thus localized loading represents a more critical (and hence realistic) test case for assessing the accuracy of any two-dimensional shell theory. From the results of Table 3, it is clear that the classical Love-Kirchhoff hypothesis is applicable only for  $R_0/h \geq 100$ . Finally, it is worth examining whether the inclusion of non-classical effects like warping of the normals to the midsurface

in a two-dimensional shell theory would be adequate for accurate analysis of locally loaded shells. For this purpose, a higher order theory based on the following displacement field is considered<sup>18,19</sup>:

$$(u, v) = (u_0, v_0) + \zeta(Q_1, Q_2) + \psi(S_1, S_2) + \zeta^3(T_1, T_2) \quad (14)$$

$$w = w_0$$

where  $u$ ,  $v$ , and  $w$  are the axial, circumferential, and radial displacements, respectively, and  $u_0$ ,  $v_0$ ,  $Q_1$ ,  $Q_2$ ,  $S_1$ ,  $S_2$ ,  $T_1$ ,  $T_2$ , and  $w_0$  are functions of the axial and circumferential coordinates alone. The  $\zeta$  is the transverse coordinate, and  $\psi$  is a zig-zag, piecewise linear function of  $\zeta$  having values of 1 and -1 alternately at the interfaces of the laminate. The inclusion of both  $\zeta^3$  and  $\psi$  in Eq. (14) leads to a close approximation of the displacement field prevailing in a laminate. The accuracy of this higher order theory has been verified for the case of a cylindrical shell subjected to sinusoidal transverse load ( $m = 1$ ,  $n = 4$ ), and results with less than 5% error have been reported for stresses and deflections at values of  $R_0/h$  as low as 10.<sup>18</sup>

Results based on this higher order theory for the present case of pinching patch loads are given in Table 4. These results correspond to the Fourier summation up to  $m = 49$  and  $n = 48$  and are values normalized with respect to the elasticity solution. From this table, it is clear that the higher order theory provides excellent results for  $R_0/h \geq 20$  and that the accuracy drops drastically as  $R_0/h$  is decreased below 20. Thus, it can be concluded that higher order theories can be used as a good alternative to rigorous three-dimensional analysis even for the case of localized loading as long as the shell under consideration is not too thick.

## Conclusion

To examine the accuracy of two-dimensional shell theories when applied to laminated composite shells subjected to local loads, benchmark results, based on three-dimensional elasticity, have been provided for a simply supported cross-ply cylindrical shell pinched by diametrically opposite local patch loads. On the basis of these results, the accuracy of the Love-Kirchhoff hypothesis and that of a refined displacement model have been examined.

## Appendix

**Table A1** Relations for  $d_r$ ,  $d_\theta$ , and  $d_z$

Item	Relation
$d_r(0, k)^a$	1 for $k = 1$ ; 0 otherwise.
$d_r(1, k)$	1 for $k = 2$ ; 0 otherwise.
$d_\theta(0, k)$	1 for $k = 3$ ; 0 otherwise.
$d_\theta(1, k)$	1 for $k = 4$ ; 0 otherwise.
$d_z(0, k)$	1 for $k = 5$ ; 0 otherwise.
$d_z(1, k)$	1 for $k = 6$ ; 0 otherwise.
For $j \geq 2$ :	
$d_r(j, k)$	$[A_1 d_r(j-4, k) + A_2 d_r(j-3, k) + A_3 d_r(j-2, k) + A_4 d_\theta(j-1, k) + A_5 d_\theta(j-2, k) + A_6 d_\theta(j-1, k) + A_7 d_z(j-3, k) + A_8 d_z(j-2, k) + A_9 d_z(j-1, k)]/A_{10}$
$d_\theta(j, k)$	$[B_1 d_r(j-2, k) + B_2 d_r(j-1, k) + B_3 d_\theta(j-4, k) + B_4 d_\theta(j-3, k) + B_5 d_\theta(j-2, k) + B_6 d_\theta(j-1, k) + B_7 d_z(j-3, k) + B_8 d_z(j-2, k)]/B_9$
$d_z(j, k)$	$[D_1 d_r(j-3, k) + D_2 d_r(j-2, k) + D_3 d_r(j-1, k) + D_4 d_\theta(j-3, k) + D_5 d_\theta(j-2, k) + D_6 d_z(j-4, k) + D_7 d_z(j-3, k) + D_8 d_z(j-2, k) + D_9 d_z(j-1, k)]/D_{10}$

<sup>a</sup> $k$  varies from 1 to 6. <sup>b</sup> $d_r = d_\theta = d_z = 0$  for  $j < 0$ .

**Table A2** Relations for  $A_1, A_2$ , etc.

Item	Relation
$A_1$	$-C_{44}s^2$
$A_2$	$-2tC_{44}s^2$
$A_3$	$C_{11}(j-2)^2 - C_{55}n^2 - C_{22} - C_{44}s^2t^2$
$A_4$	$C_{11}t(2j-3)(j-1)$
$A_5$	$(C_{55} + C_{12})n(j-2) - (C_{55} + C_{22})n$
$A_6$	$(C_{55} + C_{12})nt(j-1)$
$A_7$	$-(C_{13} + C_{44})s(j-3) - (C_{13} - C_{23})s$
$A_8$	$st[-2(C_{13} + C_{44})(j-2) - (C_{13} - C_{23})]$
$A_9$	$-(C_{13} + C_{44})st^2(j-1)$
$A_{10}$	$-C_{11}t^2j(j-1)$

**Table A3** Relations for  $B_1, B_2$ , etc.

Item	Relation
$B_1$	$-(C_{55} + C_{12})n(j-2) - (C_{55} + C_{22})n$
$B_2$	$-A_6$
$B_3$	$-C_{66}s^2$
$B_4$	$-2tC_{66}s^2$
$B_5$	$C_{55}(j-2)^2 - C_{22}n^2 - C_{55} - C_{66}s^2t^2$
$B_6$	$C_{55}t(2j-3)(j-1)$
$B_7$	$(C_{23} + C_{66})ns$
$B_8$	$(C_{23} + C_{66})nst$
$B_9$	$-C_{55}t^2j(j-1)$

**Table A4** Relations for  $D_1, D_2$ , etc.

Item	Relation
$D_1$	$(C_{13} + C_{44})s(j-3) + (C_{44} + C_{23})s$
$D_2$	$st[2(C_{13} + C_{44})(j-2) + (C_{44} + C_{23})]$
$D_3$	$-A_9$
$D_4$	$B_7$
$D_5$	$B_8$
$D_6$	$-C_{33}s^2$
$D_7$	$-2tC_{33}s^2$
$D_8$	$C_{44}(j-2)^2C_{66}n^2 - C_{33}s^2t^2$
$D_9$	$C_{44}t(2j-3)(j-1)$
$D_{10}$	$-C_{44}t^2j(j-1)$

## References

- Kapania, R. K., "A Review on the Analysis of Laminated Shells," *Journal of Pressure Vessel Technology, Transactions of the ASME*, Vol. 111, No. 2, 1989, pp. 88-96.
- Pagano, N. J., "Exact Solutions for Composite Laminates in Cylindrical Bending," *Journal of Composite Materials*, Vol. 3, No. 3, 1969, pp. 398-411.
- Pagano, N. J., "Exact Solutions for Rectangular Bidirectional Composites and Sandwich Plates," *Journal of Composite Materials*, Vol. 4, No. 1, 1970, pp. 20-34.
- Pagano, N. J., "Influence of Shear Coupling in Cylindrical Bending of Anisotropic Laminates," *Journal of Composite Materials*, Vol. 4, No. 3, 1970, pp. 330-343.
- Pagano, N. J., and Wang, A. S. D., "Further Study of Composite Laminates under Cylindrical Bending," *Journal of Composite Materials*, Vol. 5, No. 4, 1971, pp. 521-528.
- Pagano, N. J., and Hatfield, S. J., "Elastic Behaviour of Multi-layered Bidirectional Composites," *AIAA Journal*, Vol. 10, No. 7, 1972, pp. 931-933.
- Ren, J. G., "Exact Solutions for Laminated Cylindrical Shells in Cylindrical Bending," *Composites Science and Technology*, Vol. 29, No. 3, 1987, pp. 169-187.
- Ren, J. G., "Analysis of Simply-Supported Laminated Circular Cylindrical Shell Roofs," *Composite Structures*, Vol. 11, No. 4, 1989, pp. 277-292.
- Varadan, T. K., and Bhaskar, K., "Bending of Laminated Orthotropic Cylindrical Shells—An Elasticity Approach," *Composite Structures*, Vol. 17, No. 2, 1991, pp. 141-156.

<sup>10</sup>Bhaskar, K., and Varadan, T. K., "Exact Elasticity Solution for Laminated Anisotropic Cylindrical Shells," *Journal of Applied Mechanics, Transactions of the ASME*, Vol. 60, No. 1, 1993, pp. 41-47.

<sup>11</sup>Bhaskar, K., and Varadan, T. K., "A Benchmark Elasticity Solution for an Axisymmetrically Loaded Angle-Ply Cylindrical Shell," *Composites Engineering*, Vol. 3, No. 11, 1993, pp. 1065-1073.

<sup>12</sup>Bender, C. M., and Orszag, S. A., *Advanced Mathematical Methods for Scientists and Engineers*, international ed., McGraw-Hill, Singapore, 1978, pp. 61-76.

<sup>13</sup>Mirsky, I., "Three-Dimensional and Shell-Theory Analysis for Axisymmetric Vibrations of Orthotropic Shells," *Journal of the Acoustical Society of America*, Vol. 39, No. 3, 1966, pp. 549-555.

<sup>14</sup>Chou, F. H., and Achenbach, J. D., "Three-Dimensional Vibrations of Orthotropic Cylinders," *Journal of Engineering Mechanics, Transactions of the ASCE*, Vol. 98, No. 4, 1972, pp. 813-822.

<sup>15</sup>Srinivas, S., "Analysis of Laminated, Composite, Circular Cylindrical Shells with General Boundary Conditions," NASA TR R-412, April 1974.

<sup>16</sup>Misovec, A. P., and Kempner, J., "Approximate Elasticity Solution for Orthotropic Cylinder under Hydrostatic Pressure and Band Loads," *Journal of Applied Mechanics, Transactions of the ASME*, Vol. 37, No. 1, 1970, pp. 101-108.

<sup>17</sup>Bert, C. W., "Analysis of Shells," *Composite Materials*, Vol. 7, Academic Press, New York, 1975, pp. 207-258.

<sup>18</sup>Bhaskar, K., and Varadan, T. K., "An Accurate Theory of Laminated Composite Cylindrical Shells," *Journal of the Aeronautical Society of India*, Vol. 43, No. 4, 1991, pp. 307-317.

<sup>19</sup>Bhaskar, K., and Varadan, T. K., "A Higher-Order Theory for Bending Analysis of Laminated Shells of Revolution," *Computers and Structures*, Vol. 40, No. 4, 1991, pp. 815-819.

## Proceedings from the 18th Congress of the International Council of the Aeronautical Sciences

September 20-25, 1992 • Beijing, People's Republic of China

The ICAS '92 conference proceedings offer 274 exceptional papers, representing work in all branches of aeronautical science and technology. Conveniently packaged in two volumes, you will find up-to-date information on the following topics: air traffic control • performance and trajectory optimization • turbomachinery and propellers • CFD techniques and applications • maintenance systems, subsystems and manufacturing technology • lighter than air • engine/airframe integration • aircraft design concepts • passenger and crew safety • aeroelastic analysis • performance, stability and control • navigation • fault tolerant systems • fatigue • structural dynamics and control • aerodynamics • noise • combustion • wind tunnel technology • structural testing • high incidence and vortex flows • impact behavior of composites • aircraft operations and human factors • system safety and dynamics • fatigue and damage tolerance • hypersonic aircraft • avionics • supersonic and hypersonic flow • crew activity and analysis • simulators and man-machine integration • CAD/CAM and CIM, and much more

1992, 2-vol set, 2,200 pp, paper, ISBN 1-56347-046-2, AIAA Members \$130, Nonmembers \$150, Order #: 18-ICAS

Place your order today! Call 1-800/682-AIAA



American Institute of Aeronautics and Astronautics

Publications Customer Service, 9 Jay Gould Ct., P.O. Box 753, Waldorf, MD 20604  
FAX 301/843-0159 Phone 1-800/682-2422 9 a.m. - 5 p.m. Eastern

Sales Tax: CA residents, 8.25%; DC, 6%. For shipping and handling add \$4.75 for 1-4 books (call for rates for higher quantities). Orders under \$100.00 must be prepaid. Foreign orders must be prepaid and include a \$20.00 postal surcharge. Please allow 4 weeks for delivery. Prices are subject to change without notice. Returns will be accepted within 30 days. Non-U.S. residents are responsible for payment of any taxes required by their government.